Communication in Physical Sciences, 2024, 11(3): 476-484

The Efficiency of a Quantum Brayton Engine Using Wood-Saxon Potential

Oladimeji Enock Oluwole*; Umeh Emmanuel Chukwuebuka; Idundun Victory Toritseju; Koffa Durojaiye Jude; Obaje Vivian Onechojo; Uzer John Mkohol; Etim Emmanuel Edet.

Received: 10 March 2024/Accepted: 04 June 2024/Published: 10 June 2024

Abstract: *This paper investigates the efficiency of a Quantum Brayton Engine (QBE) using the Wood-Saxon (WS) potential as the working substance. The WS potential offers a more realistic model compared to the traditional Free-Particle (FP) model for studying quantum systems. The work follows the formalism established by Bender et al. (2000) to describe the QBE cycle with two isentropic and two adiabatic processes. The efficiency expression for the QBE with WS potential is derived. The derived efficiency expression showcases the dependence on the parameters of the WS potential, including depth, confinement width, and diffuseness. By taking the FP limit of the WS model, the efficiency reduces to the well-known expression for a QBE with a free particle, validating the approach. This research demonstrates the potential of the WS potential for analyzing the performance of QBE and paves the way for further exploration of more realistic models in quantum thermodynamics.*

Keywords: *Quantum thermodynamics, Wood-Saxon, Carnot cycle, Quantum heat engines, finite-engine.*

Oladimeji Enock Oluwole
Theoretical Physics Group, Department of Physics, Federal University Lokoja, Lokoja, Nigeria.
Email: nockjnr@gmail.com
Orcid id: 0000-0001-5500-8382

Umeh Emmanuel Chukwuebuka
Theoretical Physics Group, Department of Physics, Federal University Lokoja, Lokoja, Nigeria.
Email: buksjnr@gmail.com
Orcid id: 0000-0002-1875-9416

Idundun Victory Toritseju
Theoretical Physics Group, Department of Physics, Federal University Lokoja, Lokoja, Nigeria.
Email: vicidundun@gmail.com
Orcid id: 0009-0001-0552-4749

Koffa Durojaiye Jude
Theoretical Physics Group, Department of Physics, Federal University Lokoja, Lokoja, Nigeria.
Email: durojaiye.koffa@fulokoja.edu.ng
Orcid id: 0009-0002-1933-4396

Obaje Vivian Onechojo
Department of Physics, Kogi State University, Anyigba, Nigeria.
Email: vivianobaje@gmail.com
Orcid id: 0009-0007-8077-1989

Uzer John Mkohol
Department of Physics, Federal University Lokoja, Lokoja, Nigeria.
Email: john.uzer@fulokoja.edu.ng
Orcid id: 0000-0002-7412-4343

Etim Emmanuel Edet
Department of Chemical Sciences, Federal University Wukari, Nigeria.
Email: emmaetim@gmail.com
Orcid id: 0000-0001-8304-9771

1.0 Introduction

The concept of heat engines dates to antiquity, it wasn't until the Industrial Revolution in the 18th century that they were effectively harnessed into useful devices, marking a pivotal moment in the application of thermodynamics. Throughout its discovery, it has played a crucial role in shaping modern technologies, especially from the late 19th century (Bera *et al*., 2021; Bhattacharjee & Dutta, 2021). Although recently Engineers have examined different heat-engine cycles to enhance the extraction of usable work from power sources. Unfortunately, the Carnot cycle limit remains unattainable with gas-based cycles, however, theoretical models have introduced limits that achieve higher efficiency without violating any thermodynamic rules. This was possible by increasing the temperature difference in the heat engine, secondly, exploiting the physical properties of the working fluid and finally, Exploiting the chemical properties of the working fluid. These methods however have not fixed the challenges of friction that CHE faces (Rezek & Kosloff, 2006). This limitation is evident in the engine's efficiency and its overall performance, which are reduced by irreversible losses considering that not all of the energy obtained from the reservoir at a higher temperature is transformed into mechanical work (Oladimeji, Idundun, *et al*., 2024).

Due to the impact of quantum fluctuation on systems at this scale, the emergence of Quantum heat engines (QHEs), in which heat systems are reduced from microscale to nanoscale, has rendered this CHE constraint insignificant (Abah *et al*., 2012; Campisi *et al*., 2011;Oladimeji, Idundun, *et al*., 2024; Peterson *et al*., 2019; Von Lindenfels *et al*., 2019). Because engines at this scale offer a tangible setting for investigating the principles of thermodynamics in the quantum realm (Brandão *et al*., 2015; Masanes & Oppenheim, 2017). Despite this discrepancy, to understand the quantization concept of heat engines, we cannot ignore their classical analogies, such as the Carnot cycles (Fei *et al*., 2022; Martínez *et al*., 2016; Oladimeji *et al*., 2021; Türkpençe *et al*., 2017; JWang & He, 2012) Ericsson cycles, Stirling cycles, Otto cycles and Brayton cycles (J. Wang *et al*., 2007), since the thermodynamic cyclic process remains the irrespective of the size of the engine.

All engines are driven by a sort of fuel which we shall refer to as working substance. This working substance stands to be the major difference between CHEs and its QHEs counterpart. While the CHE is driven by the famously known fuels which are usually in the form of liquid i.e., diesel, gasoline, and petrol, QHEs are driven by quantum-mechanical systems, such as Free-Particle (Bender *et al*., 2000; Guzmán-Vargas *et al*., 2002; Wang & He, 2012), Harmonic Oscillators (Insinga *et al*., 2016; Jussiau *et al*., 2023; Lin & Chen, 2003; Rezek & Kosloff, 2006), Pöschl-Teller Oscillator (Oladimeji *et al*., 2021; Oladimeji, 2019), Wood-Saxon model (Oladimeji, Ibrahim, *et al*., 2024), the Morse Oscillator (E. O. Oladimeji, Idundun, *et al*., 2024) etc. The working substance has proved to have an immense effect on the performance of the quantum systems, recently we have seen several comparisons between the different types of working substances. *Oladimeji et al* (Oladimeji, Idundun, *et al*., 2024), in their work, observed that the Morse oscillator proved to be a more suitable working substance for the quantum Carnot system, they further observed the effect of the Wood-Saxon WS model in the same system, their result was finally reduced to the well know Free-Particle model for Comparism (E. O. Oladimeji, Ibrahim, *et al*., 2024).

In this work, we shall also observe the Wood-Saxon WS model as a working substance to a quantum system analogous to a Brayton cycle because this cycle is widely used in real-world applications, particularly in gas turbine engines for power generation and jet propulsion. The efficiency and its performance shall be analysed. Our study shall follow the formalism of *Bender et al* (Bender *et al*., 2000), their approach has been a tremendously useful tool to many researchers (Abe, 2011; Enock *et al*., 2021; Wang *et al*., 2012). The WS model was initially devised for studying nuclear structure and reaction properties in 1954 by R.D. Wood and D.S. Saxon (Woods & Saxon, 1954). However, in recent times, the model applied to quantum systems (Aytekin *et al*., 2013; Costa *et al*., 1999; Horchani *et al*., 2022; Xie, 2009a, 2009b), and proved to be suitable for studying nonlinearities in quantum systems and is of significant interest in understanding the performance of QHE, whose working substance is constrained within this more realistic potential model (E. O. Oladimeji, Ibrahim, *et al*., 2024).

The one-dimensional form of the potential is:

$$V(x) = \frac{-V_0}{1 + e^{\left(\frac{x-L}{a}\right)}}$$

where V_0 is the depth, L is taken to stand for the confinement width and a is the diffuseness of the interaction. The corresponding quantized eigenvalues E_n takes the form (Berkdemir *et al*., 2005):

$$E_n^{WS}(L) = -\left[\frac{V_0}{2} + \frac{(n+1)^2\hbar^2}{8mL^2} + \frac{V_0^2 mL^2}{2\hbar^2(n+1)^2}\right] \quad (1)$$

where m is the mass of the particle and $(n = 1,2,3,\ldots)$. Hence its pressure P is:

$$P_n^{WS}(L) =$$

Since the pressure exerted on the confinement is defined as:

$$P = -\left(\frac{dE}{dL}\right) \quad (3)$$

Based on this definition, it is possible to define several quantum processes analogous to those used in reversible thermodynamics. The energy supplied by the Hamiltonian's expectation value takes the place of the temperature in this situation. A process that is considered isobaric occurs when the system expands or contracts while maintaining a constant pressure, or in which the average forces acting on the container walls remain constant (Abe, 2011; Guzmán-Vargas *et al*., 2002).

This paper is structured as follows: Section 2 introduces a model of a quantum Brayton engine comprising two Isentropic and two adiabatic processes, utilizing the Woods-Saxon (WS) potential as the working medium, and derives its efficiency, η. We discussed our derived efficiency, reduced it to a well-known FP model for verification in Section 3.0 and presented our conclusions and recommendation in Section 4.0

2.0 The Brayton Cycle

The Classical Brayton engine (CBE), also known as the Joule engine or Joule-Brayton engine (Oladimeji, 2019), is a thermodynamic engine whose cycle comprises a sequence of four processes *(see Fig. 1)*: two isentropic (reversible adiabatic) processes interspersed with two isobaric (constant pressure) processes. The principle of the CBC also applies to its quantized counterpart i.e., Quantum Brayton Cycle (QBC). We will begin examining the first process i.e., the isentropic expansion phase where the pressure is constant even when the system is compressed or expanded (i.e., the rate of change of energy concerning the change in width L of the well is constant). The energy value as a function of L may be written as:

$$E(L) = \sum_{n=1}^{\infty} |a_n|^2 E_n \qquad (4)$$

where E_n is the energy spectrum (3) and the coefficients $|a_n|^2$ are constrained by the normalization condition $\sum_{n=1}^{\infty}|a_n|^2 = 1$. Given that the system at the initial state $\psi_n(x)$ of volume, L is a linear combination of eigenstates $\phi_n(x)$, the expectation value of the Hamiltonian changes concerning the change in width L of the well, then the instantaneous pressure exerted on the walls can be obtained using the relation (3).

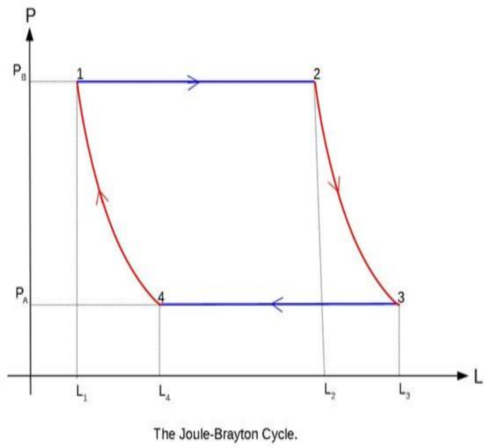

Fig. 1: The schematic representation of a quantum heat engine cycle in the plane of the width (L) and Pressure P(L). The cycle consists of two (2) isentropic and two (2) adiabatic processes (E. O. Oladimeji, 2019)

2.1.1 Process 1: Isentropic expansion

During the isentropic process, the system moves from its initial ground state $n = 0$ at point 1 (i.e., from $L = L_1$ to $L = L_2$) and is excited into the second state $n = 1$, while the expectation value of the Hamiltonian constant and the state of the system is a linear combination of its two energy eigenstates:

$$\Psi_n = a_1(L)\phi_1(x) + a_2(L)\phi_2(x)$$

where ϕ_1 and ϕ_2 are the wave functions of the first and second states respectively. The coefficients are constrained by the normalization condition$\sum_{n=1}^{\infty}|a_n|^2$, it satisfies the condition $|a_1|^2 + |a_2|^2 = 1$. The expectation value of the Hamiltonian in this state as a function of L is calculated as $E = \langle\psi|H|\psi\rangle$:

$$E(L) = -\left(\frac{V_0}{2} + \frac{\hbar^2}{8mL^2} + \frac{{V_o}^2 mL^2}{2\hbar}\right)|a_1|^2 - \left(\frac{V_0}{2} + \frac{4\hbar^2}{8mL^2} + \frac{{V_o}^2 mL^2}{8\hbar}\right)|a_2|^2$$

Recall that $|a_2|^2 = 1 - |a_1|^2$

$$E(L) = -\frac{V_0}{2} + \frac{\hbar^2}{8mL^2}[3|a_1|^2 - 4] - \frac{{V_o}^2 mL^2}{8\hbar}[6|a_1|^2 + 1] \qquad (5)$$

and pressure's value is given in terms of its definition (3):

$$P = \frac{\hbar^2}{4mL^3}[3|a_1|^2 - 4] + \frac{{V_o}^2 mL}{4\hbar}[6|a_1|^2 + 1] \qquad (6)$$

The pressure at point 1 as a function of L_1 is:

$$P_1(L) = \left(-\frac{\hbar^2}{4mL_1{}^3} + \frac{V_o{}^2 mL_1}{\hbar}\right) \tag{7}$$

The pressure during this process remains constant, therefore, $P_1 = P$, thus:

$$-\frac{\hbar^2}{4mL_1{}^3} + \frac{V_o{}^2 mL_1}{\hbar} = \frac{\hbar^2}{4mL^3}[3|a_1|^2 - 4] + \frac{V_o{}^2 mL}{4\hbar}[7|a_1|^2 + 1] \tag{8}$$

Interestingly, the Brayton cycle presents a unique relation between the values of L_1. To solve the problem, the value of the engine's width on both sides of equ. (8) is compared, thereby leading to two possible maximum values of the engine's width L during the isentropic process.

$$\frac{\hbar^2}{4mL_1{}^3} = \frac{\hbar^2}{4mL^3}[3|a_1|^2 - 4] \tag{9a}$$

And

$$\frac{V_o{}^2 mL_1}{\hbar} = \frac{V_o{}^2 mL}{4\hbar}[7|a_1|^2 + 1] \tag{9b}$$

Thus, the maximum possible value of L during this isothermal expansion is $L = L_2$, since $a_1 = 0$ at (point 2):

$$L = \left(\frac{1}{4}\right)^{\frac{1}{3}} L_1 = L_2 \tag{10a}$$

And

$$L = 4L_1 = L_2 \tag{10b}$$

Therefore.

$$L_2 = \left(\frac{1}{4}\right)^{\frac{1}{3}} L_1, 4L_1$$

2.1.2 Process 2: Adiabatic Expansion

Next, the system expands adiabatically from $L = L_2$ until $L = L_3$. During this expansion, the system remains in the second state $n = 2$ as no external energy comes into the system and the change in the internal energy equals the work performed by the walls of the well. The expectation value of the Hamiltonian is:

$$E = -\left(\frac{V_0}{2} + \frac{4\hbar^2}{8mL^2} + \frac{V_o{}^2 mL^2}{8\hbar}\right)$$

And the pressure is given by.

$$P_2(L) = \left(-\frac{\hbar^2}{mL^3} + \frac{V_o{}^2 mL}{4\hbar}\right) \tag{11}$$

The product $LP_2(L)$ in (11) is a constant that is considered the quantum analogue of the classical *adiabatic process*.

2.1.3 Process 3: Isentropic Compression

The system is in the second state $n = 1$ at point 3 (i.e., from $L = L_3$ until $L = L_4$), and it compresses isobarically. The system is compressed back to the ground state $n = 0$ as the expectation value of the Hamiltonian remains constant. Thus, the state of the system is a linear combination of its two energy eigenstates.

$$\Psi_n = b_1(L)\phi_1(x) + b_2(L)\phi_2(x)$$

The expectation value of the Hamiltonian in this state as a function of L is calculated using $E = \langle\psi|H|\psi\rangle$, which results in

$$E(L) = \sum_{n=1}^{2} |b_n|^2 E_n = |b_1|^2 E_1 + |b_2|^2 E_2$$

Recall that $|b_1|^2 = 1 - |b_2|^2$

$$E(L) = -\frac{V_0}{2} - \frac{\hbar^2}{8mL^2}[3|b_2|^2 + 1] + \frac{V_o{}^2 mL^2}{8\hbar}[6|b_2|^2 - 4] \tag{12}$$

and pressure's value is given in terms of its definition (3):

$$P = -\frac{\hbar^2}{4mL^3}[3|b_2|^2 + 1] - \frac{{V_o}^2 mL}{4\hbar}[6|b_2|^2 - 4] \tag{13}$$

The pressure at point 3 as a function of L_3 is:

$$P_3(L) = -\frac{\hbar^2}{mL_3^3} + \frac{{V_o}^2 mL_3}{4\hbar} \tag{14}$$

The pressure during this process remains constant, therefore, $P_3 = P$, thus:

$$-\frac{\hbar^2}{mL_3^3} + \frac{{V_o}^2 mL_3}{4\hbar} = -\frac{\hbar^2}{4mL^3}[3|b_2|^2 + 1] - \frac{{V_o}^2 mL}{4\hbar}[6|b_2|^2 - 4] \tag{15}$$

Just as observed at the first process of the cycle, the value of the engine's width on both sides of equ. (8) is compared, leading two possible maximum values of the engine's width L during the isentropic process.

$$-\frac{\hbar^2}{mL_3^3} = -\frac{\hbar^2}{4mL^3}[3|b_2|^2 + 1] \tag{16a}$$

And

$$\frac{{V_o}^2 mL_3}{4\hbar} = -\frac{{V_o}^2 mL}{4\hbar}[6|b_2|^2 - 4] \tag{16b}$$

Thus, the maximum possible value of L during this isothermal expansion is $L = L_4$, since $b_2 = 0$ at (point 4):

$$L = \left(\frac{1}{4}\right)^{\frac{1}{3}} L_3 = L_4 \tag{17a}$$

And

$$L = \frac{L_3}{4} = L_4 \tag{17b}$$

Therefore.

$$L_4 = (4)^{-\frac{1}{3}} L_3, (4)^{-1} L_3$$

2.1.4 Process 4: Adiabatic Compression

The system returns in the ground state $n = 0$ at point 4 (i.e., from $L = L_4$ until $L = L_1$), as it compresses adiabatically. The expectation of the Hamiltonian is given by $E = -\left(\frac{V_0}{2} + \frac{\hbar^2}{8mL^2} + \frac{{V_o}^2 mL^2}{2\hbar}\right)$ and the pressure applied to the potential well's wall is:

$$P_4(L) = \left(-\frac{\hbar^2}{4mL^3} + \frac{{V_o}^2 mL}{\hbar}\right) \tag{19}$$

2.2 Work Done in One Closed Cycle

During one closed cycle, the new work done W by the quantum heat engine is described by the area of the closed loops gotten from the processes i.e., a summation of the individual work done by each process as shown in equations (7), (11), (14) and (19).

$$W = W_{12} + W_{23} + W_{34} + W_{41} \tag{20}$$

$$W = \int_{L_1}^{L_2} P_1(L).dL + \int_{L_2}^{L_3} P_2(L).dL + \int_{L_3}^{L_4} P_3(L).dL + \int_{L_4}^{L_1} P_4(L).dL \tag{21}$$

Recall the values of L_2 and L_4 in equations (10) and (16) respectively:

$$W_{12} = \int_{\boldsymbol{L_1}}^{\boldsymbol{L_2}} \boldsymbol{P_1.dL} = \int_{L_1}^{4^{\frac{1}{3}}.L_1,4L_1} \left(-\frac{\hbar^2}{4m{L_1}^3} + \frac{{V_o}^2 mL_1}{\hbar}\right).dL = F_1L_1\left(4^{\frac{1}{3}} - 1, 4 - 1\right)$$

$$W_{12} = F_1L_1\left(4^{\frac{1}{3}} - 1, 3\right) \tag{22}$$

$$W_{23} = \int_{\boldsymbol{L_2}}^{\boldsymbol{L_3}} \boldsymbol{P_2.dL} = \int_{4^{\frac{1}{3}}.L_1,4L_1}^{L_3} \left(-\frac{\hbar^2}{mL^3} + \frac{{V_o}^2 mL}{4\hbar}\right).dL = \int_{4^{\frac{1}{3}}\boldsymbol{L_1}}^{\boldsymbol{L_3}} -\frac{\hbar^2}{mL^3}.dL + \int_{\boldsymbol{4L_1}}^{\boldsymbol{L_3}} \frac{{V_o}^2 mL}{4\hbar}.dL$$

$$W_{23} = F_1L_1\left(\frac{4^{\frac{1}{3}}}{2}, \frac{-4}{2}\right) + F_3L_3\left(\frac{-1}{2}, \frac{1}{2}\right) \tag{23}$$

$$W_{34} = \int_{L_3}^{L_4} \boldsymbol{P_3}.\boldsymbol{dL} = \int_{L_1}^{4^{\frac{-1}{3}}.L_3,4^{-1}L_3} \left(-\frac{\hbar^2}{mL_3{}^3} + \frac{V_o{}^2 mL_3}{4\hbar}\right).dL = F_3L_3\left(\left(4^{\frac{-1}{3}}, 4^{-1}\right) - 1\right)$$

$$W_{34} = F_3L_3\left(4^{\frac{-1}{3}} - 1, -\frac{3}{4}\right) \tag{24}$$

$$W_{41} = \int_{L_4}^{L_1} \boldsymbol{P_4}.\boldsymbol{dL} = \int_{4^{\frac{-1}{3}}.L_3,4^{-1}L_3}^{L_1} \left(-\frac{\hbar^2}{4mL^3} + \frac{V_o{}^2 mL}{\hbar}\right).dL = \int_{4^{\frac{-1}{3}}L_3}^{L_1} -\frac{\hbar^2}{4mL^3}.dL + \int_{4^{-1}L_3}^{L_1} \frac{V_o{}^2 mL}{\hbar}.dL$$

$$W_{41} = F_3L_3\left(\frac{4^{\frac{-1}{3}}}{2}, \frac{-4^{-1}}{2}\right) + F_1L_1\left(\frac{-1}{2}, \frac{1}{2}\right) \tag{25}$$

Combining equations $W_{23}$and W_{41}, we have that.

$$W_{23} + W_{41} = F_1L_1\left(\frac{4^{\frac{1}{3}}}{2}, \frac{-4}{2}\right) + F_3L_3\left(\frac{-1}{2}, \frac{1}{2}\right) + F_3L_3\left(\frac{4^{\frac{-1}{3}}}{2}, \frac{-4^{-1}}{2}\right) + F_1L_1\left(\frac{-1}{2}, \frac{1}{2}\right)$$

$$W_{23} + W_{41} = F_1L_1\left(\frac{4^{\frac{1}{3}} - 1}{2}, \frac{-3}{2}\right) + F_3L_3\left(\frac{4^{\frac{-1}{3}} - 1}{2}, \frac{3}{8}\right) \tag{26}$$

Thus, the total work-done W by the engine in one cycle is:

$$W = F_1L_1\left(\frac{3}{2}(4^{\frac{1}{3}} - 1), \frac{3}{2}\right) + F_3L_3\left(\frac{3}{2}(4^{\frac{-1}{3}} - 1), -\frac{2}{8}\right) \tag{27}$$

The efficiency η of a heat engine is defined as.

$$\eta = \frac{W}{Q_H}$$

given that Q_H is the quantity of heat in the hot reservoir and W is the work performed by the classical heat engine which is analogous to the energy absorbed by the quantum engine during the isothermal expansion. The heat input $Q_H = W_{12} + \Delta E_{12}$; where W_{12} and ΔE_{12} are the work performed and the change in the internal energy along the Isentropic branch. Where:

$$\Delta E_{12} = F_1L_1\left(\frac{4^{\frac{1}{3}} - 1}{2}, \frac{-3}{2}\right) \tag{28}$$

And the work W_{12} is given by the first term of the work-done W. Thus, the heat input Q_H can be expressed as

$$Q_H = F_1L_1\left(4^{\frac{1}{3}} - 1, 3\right) + F_1L_1\left(\frac{4^{\frac{1}{3}} - 1}{2}, \frac{-3}{2}\right) \tag{29}$$

$$Q_H = F_1L_1\left(\frac{3}{2}(4^{\frac{1}{3}} - 1), \frac{3}{2}\right) \tag{30}$$

Therefore, the efficiency η of a quantum heat engine obtained by considering a two-state system in a WS potential model is given by.

$$\eta = \frac{F_1L_1\left(\frac{3}{2}(4^{\frac{1}{3}} - 1), \frac{3}{2}\right) + F_3L_3\left(\frac{3}{2}(4^{\frac{-1}{3}} - 1), -\frac{2}{8}\right)}{F_1L_1\left(\frac{3}{2}(4^{\frac{1}{3}} - 1), \frac{3}{2}\right)}$$

$$\eta = 1 - \frac{F_3L_3\left(\frac{3}{2}\left(1 - 4^{\frac{-1}{3}}\right), \frac{2}{8}\right)}{F_1L_1\left(\frac{3}{2}(4^{\frac{1}{3}} - 1), \frac{3}{2}\right)} \tag{31}$$

3.0 Result And Discussion

The WS-potential of recent has been a promising model in analysing low-dimensional systems and more importantly its application in Quantum engines. It has proven to be a more realistic fuel to drive Quantum systems due to its interaction with the potential width L which mimics the way of classical heat engine. To verify our derived result in equ. (31), let's consider the FP-limit of the WS model, where the depth of the potential energy well $V_0 \to 0$. The efficiency becomes:

$$\eta_{FP} = 1 - \frac{F_3^* L_3 \left(\frac{3}{2}\left(1 - 4^{\frac{-1}{3}}\right)\right)}{F_1^* L_1 \left(\frac{3}{2}\left(4^{\frac{1}{3}} - 1\right)\right)} = 1 - \frac{F_3^* L_3}{F_1^* L_1}\left(\frac{4^{\frac{1}{3}} - 1}{4^{\frac{1}{3}}}\right)\left(\frac{1}{4^{\frac{1}{3}} - 1}\right)$$

Where $F_1^* = -\frac{\hbar^2}{4mL_1{}^3}, F_3^* = -\frac{\hbar^2}{mL_3{}^3}$

$$\eta_{FP} = 1 - \frac{F_3^* L_3}{F_1^* L_1}\left(\frac{1}{4^{\frac{1}{3}}}\right)$$

Our derived efficiency is indicated to be the same as that of other research (Guzmán-Vargas *et al*., 2002; E. O. Oladimeji, 2019), proofing that the energy efficiency of all engine are the same as our engine remains analogous with classical Brayton engine.

4.0 Conclusion

This research explores the efficiency of a Quantum Brayton Engine (QBE) that utilizes the Wood-Saxon (WS) potential as its working fluid. The WS potential provides a more realistic representation compared to the standard Free-Particle (FP) model for quantum systems.

The study employs the established formalism by Bender *et al*. (2000) to define the QBE cycle with two isentropic and two adiabatic processes. The efficiency expression for the QBE *showed that the* derived efficiency formula incorporates the influence of the WS potential's parameters, such as depth, confinement width, and diffuseness. *Also, with the simplification of* the WS model to the FP limit, the efficiency expression aligns with the known efficiency for a QBE with a free particle, validating the employed approach.

This research demonstrates the potential of the WS potential for analyzing the performance of QBE. It opens doors for further exploration of more intricate and realistic models in the field of quantum thermodynamics. *The following recommendations are hereby proposed for future study*

(i) Analyzing the impact of varying the WS potential parameters on the QBE's efficiency.

(ii) Comparing the performance of the WS-based QBE with other models employing different working fluids.

(iii) Investigating the potential for optimization of the QBE design based on the WS potential characteristics.

5.0 References

Abah, O., Roßnagel, J., Jacob, G., Deffner, S., Schmidt-Kaler, F., Singer, K., & Lutz, E. (2012). Single-ion heat engine at maximum power. *Physical Review Letters*, 109, 120, https://doi.org/10.1103/PhysRevLett.109.203006

Abe, S. (2011). Maximum-power quantum-mechanical Carnot engine. *Physical Review E - Statistical, Nonlinear, and Soft Matter Physics*, *83*, 4, pp. 1–3. https://doi.org/10.1103/PhysRevE.83.041117

Aytekin, O., Turgut, S., Üstoğlu Ünal, V., Akşahin, E., & Tomak, M. (2013). Nonlinear optical properties of a Woods–Saxon quantum dot under an electric field. *Physica E: Low-Dimensional Systems and Nanostructures*, 54, 2, pp. 257–261. https://doi.org/10.1016/j.physe.2013.06.004

Bender, C. M., Brody, D. C., & Meister, B. K. (2000). Quantum mechanical Carnot engine. *Journal of Physics A: Mathematical and General*, 33, 24, pp. 4427–4436. https://doi.org/10.1088/0305-4470/33/24/302

Bera, M. L., Julià-Farré, S., Lewenstein, M., & Bera, M. N. (2021). Quantum heat engines with carnot efficiency at maximum power.

ArXiv, 1–11. http://arxiv.org/abs/2106.01193

Berkdemir, C., Berkdemir, A., & Sever, R. (2005). Polynomial solutions of the Schrödinger equation for the generalized Woods-Saxon potential. *Physical Review C*, 72, 2, 027001. https://doi.org/10.1103/PhysRevC.72.027001

Bhattacharjee, S., & Dutta, A. (2021). Quantum thermal machines and batteries. In *European Physical Journal B*, 94, 12, https://doi.org/10.1140/epjb/s10051-021-00235-3

Brandão, F., Horodecki, M., Ng, N., Oppenheim, J., & Wehner, S. (2015). The second laws of quantum thermodynamics. *Proceedings of the National Academy of Sciences*, 112, 11, pp. 3275–3279. https://doi.org/10.1073/pnas.1411728112

Campisi, M., Hänggi, P., & Talkner, P. (2011). Erratum: Quantum fluctuation relations: Foundations and applications (Reviews of Modern Physics). In *Reviews of Modern Physics*, 83, 3, pp. . 771–791). https://doi.org/10.1103/RevModPhys.83.771

Costa, L. S., Prudente, F. V., Acioli, P. H., Neto, J. J. S., & Vianna, J. D. M. (1999). A study of confined quantum systems using the Woods-Saxon potential. *Journal of Physics B: Atomic, Molecular and Optical Physics*, 32, 10, pp. 2461–2470. https://doi.org/10.1088/0953-4075/32/10/313

Enock, O., Emmanuel, U., & Oghenetega, A. (2021). The efficiency of simple Quantum Engine Stirling and Ericsson cycle. *Confluence Journal of Pure and Applied Sciences*, 4, 1, pp. 111–119. https://doi.org/10.48550/arXiv.2010.01581

Fei, Z., Chen, J.-F., & Ma, Y.-H. (2022). Efficiency statistics of a quantum Otto cycle. *Physical Review A*, 105, 2, https://doi.org/10.1103/physreva.105.022609

Guzmán-Vargas, L., Granados, V., & Mota, R. D. (2002). Efficiency of simple quantum engines: The Joule-Brayton and Otto cycles. *AIP Conference Proceedings*, 643, pp. 291–296. https://doi.org/10.1063/1.1523819

Horchani, R., Al-Shafii, S., Al-Hashimi, N., Ikot, A. N., Okon, I. B., Okorie, U. S., Duque, C. A., & Oladimeji, E. O. E. O. (2022). Bound state solutions and thermal properties of the N-dimensional Schrödinger equation with Varshni plus Woods-Saxon potential via Nikiforov-Uvarov method. *Journal of Theoretical and Applied Physics*, 16, 4,. https://doi.org/10.30495/jtap.162243

Insinga, A., Andresen, B., & Salamon, P. (2016). Thermodynamical analysis of a quantum heat engine based on harmonic oscillators. *Physical Review E*, 94, 1, 012119. https://doi.org/10.1103/PhysRevE.94.012119

Jussiau, É., Bresque, L., Auffèves, A., Murch, K. W., & Jordan, A. N. (2023). Many-body quantum vacuum fluctuation engines. *Physical Review Research*, 5, 3, 033122. https://doi.org/10.1103/PhysRevResearch.5.033122

Lin, B., & Chen, J. (2003). Performance analysis of an irreversible quantum heat engine working with harmonic oscillators. *Physical Review E*, 67, 4, 046105. https://doi.org/10.1103/PhysRevE.67.046105

Martínez, I. A., Roldán, E., Dinis, L., Petrov, D., Parrondo, J. M. R., & Rica, R. A. (2016). Brownian Carnot engine. *Nature Physics*, 12, 1, pp. 67–70. https://doi.org/10.1038/nphys3518

Masanes, L., & Oppenheim, J. (2017). A general derivation and quantification of the third law of thermodynamics. *Nature Communications*, 8, pp. 1–7. https://doi.org/10.1038/ncomms14538

Oladimeji, E. O. (2019). The efficiency of quantum engines using the Pöschl – Teller like oscillator model. *Physica E: Low-Dimensional Systems and Nanostructures*, 111, pp. 113–117. https://doi.org/10.1016/j.physe.2019.03.002

Oladimeji, E. O., Ibrahim, T. T., Ikot, A. N., Koffa, J. D., Edogbanya, H. O., Umeh, E. C., & Audu, J. (2024). The efficiency of Quantum Mechanical Carnot Engine using the Woods Saxon model. *Sule Lamido University Journal of Science & Technology*, 9, 1, 2, https://doi.org/10.48550/arXiv.2203.02564.

Oladimeji, E. O., Idundun, V. T., Umeh, E. C., Ibrahim, T. T., Ikot, A. N., Koffa, J. D., & Audu, J. O. (2024). The Performance Analysis of a Quantum Mechanical Carnot-Like Engine Using Diatomic Molecules. *Journal of Low Temperature Physics*, 0123456789.

https://doi.org/10.1007/s10909-024-03114-0

Oladimeji, E., Owolabi, S., & Adeleke, J. (2021). The Pöschl-Teller like description of Quantum-Mechanical Carnot engine. *Chinese Journal of Physics*, *70,* pp. 151–156. https://doi.org/10.1016/j.cjph.2021.01.004

Peterson, J. P. S., Batalhão, T. B., Herrera, M., Souza, A. M., Sarthour, R. S., Oliveira, I. S., & Serra, R. M. (2019). Experimental Characterization of a Spin Quantum Heat Engine. *Physical Review Letters*, 123, 24, . https://doi.org/10.1103/PhysRevLett.123.240601

Rezek, Y., & Kosloff, R. (2006). Irreversible performance of a quantum harmonic heat engine. *New Journal of Physics*, 8, 5, pp. 83–83. https://doi.org/10.1088/1367-2630/8/5/083

Türkpençe, D., Altintas, F., Paternostro, M., & Müstecaplioğlu, Ö. E. (2017). A photonic Carnot engine powered by a spin-star network. *EPL (Europhysics Letters)*, 117, 5, 50002. https://doi.org/10.1209/0295-5075/117/50002

Von Lindenfels, D., Gräb, O., Schmiegelow, C. T., Kaushal, V., Schulz, J., Mitchison, M. T., Goold, J., Schmidt-Kaler, F., & Poschinger, U. G. (2019). Spin Heat Engine Coupled to a Harmonic-Oscillator Flywheel. *Physical Review Letters*, 123, 8, https://doi.org/10.1103/PhysRevLett.123.080602

Wang, J., & He, J. (2012). Optimization on a three-level heat engine working with two noninteracting fermions in a one-dimensional box trap. *Journal of Applied Physics*, 111, 4, https://doi.org/10.1063/1.3681295

Wang, J., He, J., & Xin, Y. (2007). Performance analysis of a spin quantum heat engine cycle with internal friction. *Physica Scripta*, 7, 2, pp. 227–234. https://doi.org/10.1088/0031-8949/75/2/018

Wang, R., Wang, J., He, J., & Ma, Y. (2012). Performance of a multilevel quantum heat engine of an ideal <math display="inline"> <mi>N</mi> </math> -particle Fermi system. *Physical Review E*, 86, 2, 021133. https://doi.org/10.1103/PhysRevE.86.021133

Woods, R. D., & Saxon, D. S. (1954). Diffuse Surface Optical Model for Nucleon-Nuclei Scattering. *Physical Review*, 95, 2, pp. 577–578. https://doi.org/10.1103/PhysRev.95.577

Xie, W. (2009a). A study of an exciton in a quantum dot with Woods-Saxon potential. *Superlattices and Microstructures*, 46, 4, pp. 693–699. https://doi.org/10.1016/j.spmi.2009.06.013

Xie, W. (2009b). A study of two confined electrons using the Woods–Saxon potential. *Journal of Physics: Condensed Matter*, 21, 11, 115802. https://doi.org/10.1088/0953-8984/21/11/115802

Compliance with Ethical Standards Declarations

The authors declare that they have no conflict of interest.

Data availability

All data used in this study will be readily available to the public

Availability of data and materials

The publisher has the right to make the data public.

Competing interests

The authors declared no conflict of interest.

Funding

The authors declared no source of funding.

Authors' contributions

Oladimeji Enock, Umeh Emmanuel and Idundun Victory developed the conceptualization. Koffa Durojaiye and Obaje Vivian resolved the equations. Uzer John; Etim Emmanuel did the proofreading in addition to interpreting the solution.